

Performance Evaluation of Tall Buildings using Optimized Tuned Mass Damper

Mohammad Shamim Miah*

Department of Civil Engineering, International University of Business Agriculture and Technology, Dhaka 1230, Bangladesh

Received: November 21, 2020, Revised: December 19, 2020, Accepted: December 22, 2020, Available Online: December 30, 2020

ABSTRACT

This study investigates the performance of tall buildings using tuned mass damper (TMD) under dynamic loads such as harmonic loads, and the Loma Prieta Earthquake 1989 data. The numerical investigations are performed by considering a sixteen-storied dynamical system. To do this end, the aforementioned system is considered to be uncontrolled (meaning no damper is used) and a controlled case is assumed where a TMD is placed on the top floor. TMD performance mainly relies on the set of parameters (mass ratio, damping ratio, and stiffness). In reality, the tuning process of those parameters take serious effort and gets worse with the complicity of the structure. Hence to obtain better performance of the TMD the damping ratio and the frequency of the TMD are optimized by using unconstrained derivative-free method. Finally, the uncontrolled and controlled performance of the sixteen-storied structure has been evaluated and compared. The results show that the dynamical response of the studied problem can be reduced significantly via the use of optimized parameters.

Keywords: Optimization; Vibration mitigation; TMD; Tall-buildings; Dynamic loads.



This work is licensed under a [Creative Commons Attribution-Non Commercial 4.0 International License](https://creativecommons.org/licenses/by-nc/4.0/).

1. Introduction

The dynamic response of any buildings, bridges, towers, and power-plants are difficult to deal with due their complex phenomena. However, the safety of the aforementioned structures is not an option but must due to their importance in the society. Though there are many alternatives (passive, active, hybrid, etc.) available in existing literature [1]-[5] but still improvements are essential. The improvements of available alternatives are essential to fulfill the upcoming uncertain challenges and events such as gale thrust, and earthquake [5]. The tuned-mass damper (TMD) falls into the passive category. And TMD is one of the oldest vibration mitigation system and implemented to many existing structures [4]. For instance, the London Millennium Bridge, Tehran International Tower in Iran, Taipei 101 in Taiwan, Trump World Tower in USA, Tokyo Skytree, Burj Khalifa in UAE, and so on have adopted TMD to reduce unwanted vibration [6]. The performance of any TMD depends on the proper selection of its parameters. Many [7]-[12] have studied the role of TMD parameters such as mass ratio, stiffness, and damping have been reported their selection or tuning process. TMDs are widely used in various types of structures due to their simple structure and reasonable performance among other alternatives [11]. Typically, the performance of any TMD relies on the best selected parameters through tuning process. To tackle drawbacks of manual tuning process, [13]-[21] works have done the optimizing of TMDs properties using genetic algorithm. Initial works of modern TMD functionality was surfaced by Den Hartog [7]. Afterward, many [1], [11], [14] have developed different types of TMD.

Over the last few decays, many alternatives of TMD and its variations have been developed and implemented, such as active control systems, semi-active control systems, and hybrid control systems [1]-[6]. And early mentioned works have reported the superior performances of those controlling systems. However,

there are underlying drawbacks of those controlling systems as most of the controlling technique (e.g., active) requires electric power, and that is quite difficult to ensure during an extreme event such as earthquake [2], [5]. And this is one of the most important issues about TMD that it does not require any electric power for its operation during an extreme event. Hence it can be operated even during an extreme event without putting much extra effort [4], [8], [11]. In general, the selection of TMD parameters take into a complicated situation when the structures are complex [15]. And when the structures are taller, the process gets harder to deal with; hence to overcome such issue optimization is preferable instead of manual tuning [19]. Therefore, an optimization will assist to overcome the drawbacks of sub-optimal tuning of parameters.

This study aims to evaluate the performance of TMD under earthquake and harmonic type dynamic loads. Additionally, the possibility of optimization of damping ratio and the frequency of the TMD has been investigated. In order to perform numerical analyses, the compact formulation of state-space is adopted. Additionally, the unconstrained derivative-free method was employed to perform the optimization. For numerical investigations, a sixteen-storied dynamical system is considered. Finally, the results of controlled and uncontrolled systems are compared.

2. Formulation and Description of the Problem

Usually, the dynamical systems are considered to be lumped-mass system and modeled as mass-spring-dashpot systems (see Fig. 1. And the dynamical systems are written into individual equation of motion by employing Newton's Second Law of classical mechanics. However, it is quite difficult to deal with several equations as each degree-of-freedom will provide an equation of motion. Hence in order to perform the investigations, those equations of motion need to bring into matrix-vector form. A dynamical system coupled with a TMD can be described as,

*Corresponding Author Email Address: mmshamim@iubat.edu

$$\begin{aligned}
\underbrace{\begin{bmatrix} m_1 & 0 & 0 \\ 0 & \ddots & 0 \\ 0 & 0 & m_n \end{bmatrix}}_M \ddot{u}(t) + \underbrace{\begin{bmatrix} c_1 + c_2 & -c_2 & 0 \\ -c_2 & \ddots & 0 \\ 0 & 0 & c_n \end{bmatrix}}_C \dot{u}(t) \\
+ \underbrace{\begin{bmatrix} k_1 + k_2 & -k_2 & 0 \\ -k_2 & \ddots & 0 \\ 0 & 0 & k_n \end{bmatrix}}_K u(t) \\
= -\Gamma \ddot{u}_g(t) + YF(t)
\end{aligned} \quad (1)$$

where M represents the mass matrix ($n \times n$), C is the damping matrix ($n \times n$), K indicates the stiffness matrix ($n \times n$), n is the number of degree-of-freedom, \ddot{u} , \dot{u} , and u are the acceleration, velocity, and displacement vectors, respectively, and they have a size of $n \times 1$, t is the time vector, \ddot{u}_g means the input disturbance, F is the TMD control force, Γ control the input excitation location, Y locates the position of TMD. Note the second term on the right-hand side of the equation that will not be available if there is no control force applied to the system.

The free-body-diagrams of every degree of freedom (e.g., floor) are essential to derive the individual floor's equation of motion. Sample free-body-diagrams of the 1st, 5th, and top floor with TMD are depicted in Fig. 1 (b-d), respectively. And all of the equations are then compiled into a compact form known as state-space formulation. The above-mentioned equation (Eq. (1)) can be further written into state-space form. The state-space formulation is accompanied with two main equations, (i) the system equation Eq. (2), and (ii) the observation equation Eq. (3). The system equation contains all the information related to consider dynamical system including input excitation and control force.

$$\dot{X}(t) = AX(t) + BU(t) \quad (2)$$

Where A is the system matrix, B indicates the input matrix, X is the state vector, and U contains the input excitation and control force information.

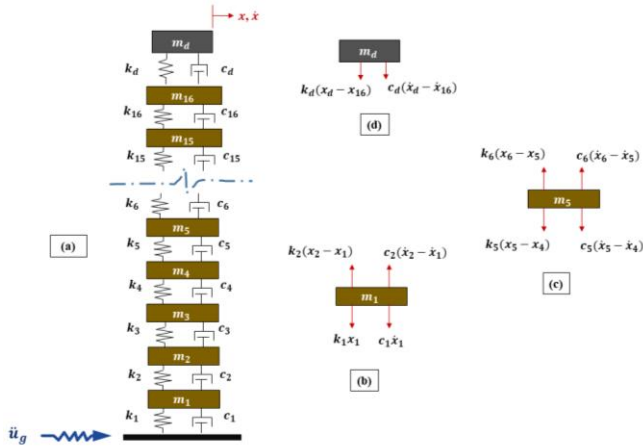


Fig. 1 The dynamical system: (a) the lumped-mass model, (b) free-body-diagram of 1st floor, (c) free-body-diagram of 5th floor, and (d) free-body-diagram of top floor.

While the observation equation describes about the information what ones want to measure or observe. Hence this equation needs to be modified as per the designer desire (based on what he/she wants to measure).

$$y(t) = CX(t) + DU(t) \quad (3)$$

where C is the output matrix, D indicates the feedthrough matrix, y is the output vector.

The parameters of the TMD has been tuned in a hybrid manner, more specifically, the mass ratio (μ) of the TMD is done through conventional procedure. The mass ratio of the TMD is defined as the ratio of the mass of the TMD to the targeted floor mass of the structure. While the frequency of the TMD has been defined as,

$$\omega_d = \delta \times \omega_n^{tar} \quad (4)$$

where ω_d is the frequency of the TMD, ω_n^{tar} is the targeted natural frequency of the structure, δ is the parameter needs to be tuned or determined to obtain an optimal frequency of the TMD. Further, the damping ratio of the TMD has been given by,

$$C_d = 2(\alpha\tau^{tmd})\omega_d \quad (5)$$

where α is a parameter links to the mass ratio of the TMD (but determined by the optimization algorithm), τ^{tmd} is the damping ratio of the TMD.

3. The Optimization Algorithm

A brief overview of the applied optimization algorithm is provided in this section. Assume the objective function of a problem is given by,

$$\min_x f(x) \rightarrow x \in \mathbb{R}^n$$

Then the iteration of the Nelder-Mead algorithm follows as shown below,

(i) Order: Order the $n + 1$ vertices to satisfying the following rules

$$f(x_1) \leq f(x_2) \leq \dots \leq f(x_{n+1})$$

(ii) Reflect: determine the reflection point x_r

$$f_r = f(x_r) = \bar{x} + \rho(\bar{x} - x_{n+1})$$

$$= (1 + \rho)\bar{x} - \rho(x_{n+1}); \quad \bar{x} = \sum_{i=1}^n \frac{x_i}{n}$$

(iii) Expand: If $f_r < f_1$ determine the expansion point x_e

$$\begin{aligned}
f_e = f(x_e) &= \bar{x} + \chi\rho(\bar{x} - x_{n+1}) \\
&= (1 + \rho\chi)\bar{x} - \rho\chi(x_{n+1})
\end{aligned}$$

If $f_e < f_r$ accept the expansion point x_e

(iv) Contract: if $f_r \geq f_n$ then perform a contraction between \bar{x} and the better x_{n+1} and x_r

Outside: if $f_n \leq f_r < f_{n+1}$ then calculate x_c , perform an outside contraction

$$\begin{aligned}
f_c = f(x_c) &= \bar{x} + \gamma(x_r - \bar{x}) = \bar{x} + \rho\gamma(\bar{x} - x_{n+1}) \\
&= (1 + \rho\gamma)\bar{x} - \rho\gamma x_{n+1}
\end{aligned}$$

If $f_c \leq f_r$ accept the contraction point x_c , and terminate the iteration; otherwise, go to perform a shrink.

Inside: if $f_r \geq f_{n+1}$ then calculate x_{cc} , perform an inside contraction

$$f_{cc} = f(x_{cc}) = \bar{x} - \gamma(\bar{x} - x_{n+1}) = (1 - \gamma)\bar{x} + \gamma x_{n+1}$$

If $f_{cc} < f_{n+1}$ accept the contraction point x_{cc} , and terminate the iteration; otherwise, go to perform a shrink.

Perform a shrink step: Evaluate f_n at the n points

$$v_i = x_1 + \sigma(x_i - x_1), \quad i = 2, \dots, n + 1$$

Interested reader may obtain detail information about basic formulation of the employed optimization algorithm through [21].

4. Results and Discussion

The numerical investigations are performed by employing MATLAB and SIMULINK. It is mentioned that a sixteen-storied structure is considered for this study. And the response of the structure is evaluated subjected to harmonic type load and the Loma Prieta Earthquake 1989 data. The input excitations (a) Loma Prieta Earthquake 1989, and (b) harmonic loads are presented in Fig. 2. It is important to note that the input excitations are going to influence the output of the structure. That is the reason of choosing different excitations force to excite the selected system. The whole simulations are performed for both uncontrolled and controlled structure for earthquake and harmonic loads.

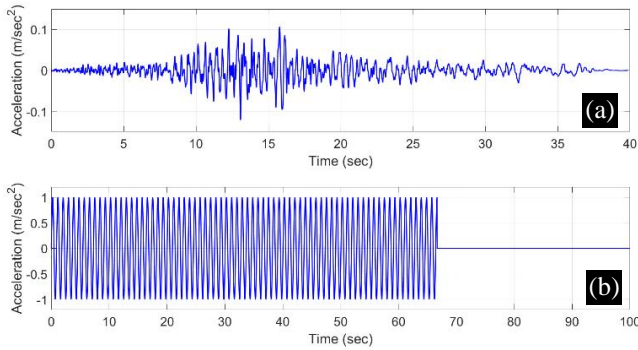


Fig. 2 The input excitations: (a) Loma Prieta Earthquake, and (b) harmonic loads.

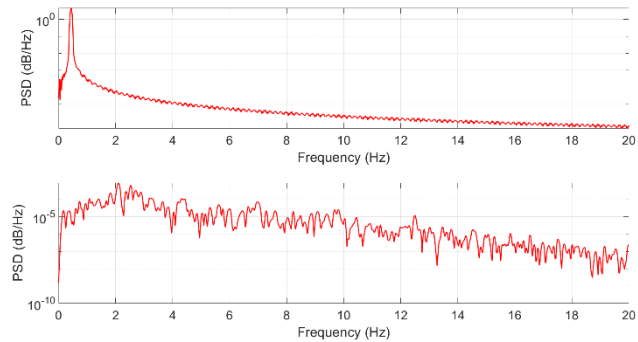


Fig. 3 The power spectral density of the input excitations.

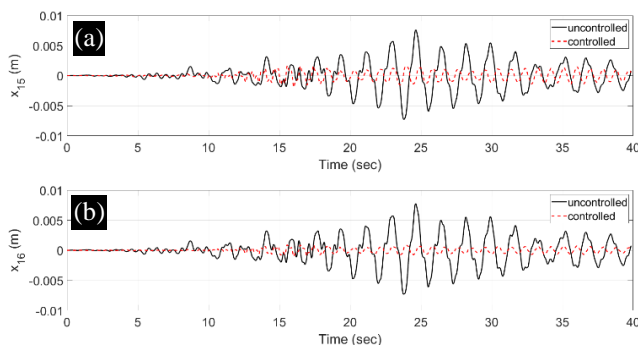


Fig. 4 Comparison of uncontrolled and controlled response of 15th and 16th floors under Loma Prieta earthquake.

The duration of the excitations 40 sec for earthquake and 100 sec for the harmonic load, also can be found in Fig. 2. In order to understand about the governing frequency (see the peaks) of the excitations, the power spectral density (PSD) of both input

excitations are depicted in Fig. 3. The structure is assumed to have a mass in every floor of 50×10^3 kg and stiffness is assumed to have 70000×10^3 N/m, and the damping coefficients are assumed to 1.3334×10^3 N-s/m. It is mentioned earlier optimization was performed by adopting unconstrained derivative-free method.

Hence the simulations are performed using those optimized values of τ^{tmd} & δ instead of manual tuning. And the parameter α is assumed to be $0.04 \times m^{tar}$, where m^{tar} is considered to be modal mass of the targeted mode. However, that does not affect the uncontrolled structural response except the changes of input excitations e.g., earthquake, harmonic. To evaluate the performance of the optimized values of the TMD, the top two floors (x_{15} and x_{16}) displacements are compared for controlled and uncontrolled scenarios. Fig. 4 shows the comparison of the controlled (dotted red-line) and uncontrolled (black-line) displacements for the Loma Prieta 1989 earthquake data. It is visible that the response of the structure has been mitigated effectively.

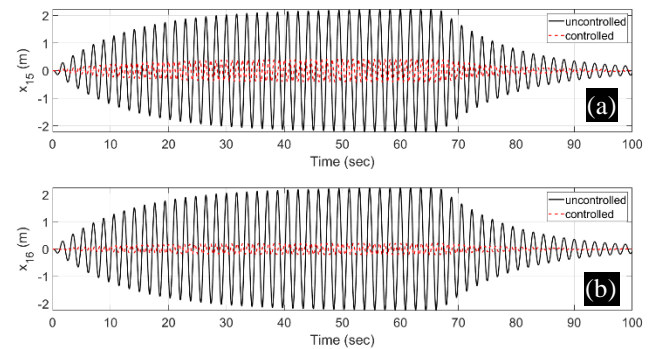


Fig. 5 Comparison of uncontrolled and controlled response of 15th and 16th floors subjected to harmonic load.

Afterward, the structure was hit by the harmonic load and the response of the uncontrolled and controlled structures are compared in Fig. 5. The dotted red line indicates the controlled response and the black line represents uncontrolled case. From the figure it can be stated that the vibration was reduced significantly.

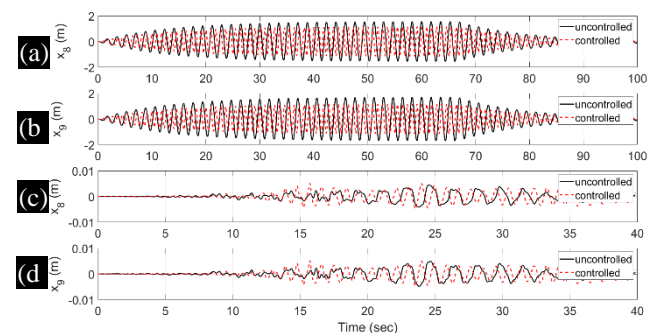


Fig. 6 The response of 8th and 9th floors subjected to harmonic load (a-b) and earthquake loads (c-d).

Furthermore, the maximum displacements of every floor have been evaluated and depicted in Fig. 5. The left figure (see Fig. 5 (a)) shows the output of the structures due to earthquake and the right figure (see Fig. 5 (b)) exhibits the response under harmonic load. The response of 8th and 9th floors are presented in Fig. 6 and it is visible that those floors are suffering with abrupt deformation. This phenomenon is also noticeable in Fig. 7.

It can be found that the maximum displacements of every floor have reduced for both earthquake and harmonic loads. It also visible in Fig. 7 (a) that the structure will reach in a position where it will face nonlinear/large deformation as a result structure may fail partly/fully. Hence such situation will demand more safety to survive from extreme loads. However, the early mentioned situation also may occur even when harmonic type load hits the structure totally an unexpected way as shown in Fig. 7 (b).

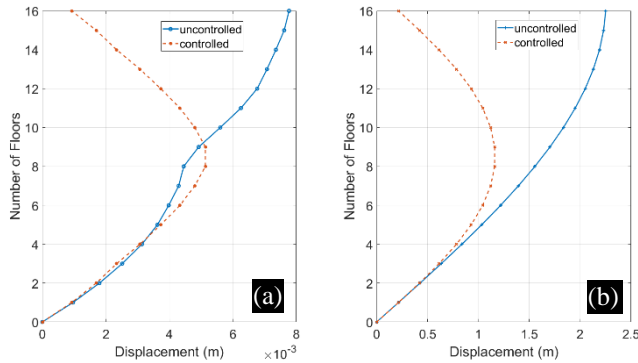


Fig. 7 The uncontrolled and controlled response of all of the floors subjected: (a) Loma Prieta earthquake, and (b) harmonic load.

5. Conclusion

The performance of a sixteen-storied dynamical system with and without TMD are investigated. Further, the frequency and the damping ratio of the TMD has been optimized to obtain better performance. An unconstrained derivative-free optimization method is used to perform the optimization. The outcome of the study shows that the optimization may be suitable for tall-buildings as complexities are not limited to the structure but also from input excitation and model descriptions. Hence to deal with such uncertain situation optimization of any tuning parameter such as mass ratio, damping ratio and stiffness of the TMD will perform better in comparison to sub-optimal/manual tuning. The future direction of this study will focus into the system identification to deal with more complex problems.

References

- [1] Elias, S. and Matsagar, V., 2017. Research developments in vibration control of structures using passive tuned mass dampers. *Annual Reviews in Control*, 44, pp.129-156.
- [2] Dyke, S.J., Spencer Jr, B.F., Belknap, A.E., Ferrell, K.J., Quast, P. and Sain, M.K., 1994, August. Absolute acceleration feedback control strategies for the active mass driver. *In Proc. First World Conference on Structural Control* (pp. 51-60).
- [3] Chu, S.Y., Soong, T.T. and Reinhorn, A.M., 2005. Active, hybrid, and semi-active structural control: A design and implementation handbook. New York: Wiley.
- [4] Miah, M.S., 2011. Dynamic Behavior of Bridge with New Innovative Type Spherical Elastomeric Bearing. *Kunsan National University*, Kunsan, South Korea, pp.1-122.
- [5] Miah, M.S., Chatzi, E.N., Dertimanis, V.K. and Weber, F., 2017. Real-time experimental validation of a novel semi-active control scheme for vibration mitigation. *Structural Control and Health Monitoring*, 24(3), p.e1878.
- [6] Wikipedia. Tuned mass damper, Available: https://en.wikipedia.org/wiki/Tuned_mass_damper (Accessed on 29 September 2020).
- [7] Hartog, J. P. D. (1947). Mechanical vibrations, 3rd ed., McGraw-Hill, New York.
- [8] Warburton, G.B., 1981. Optimum absorber parameters for minimizing vibration response. *Earthquake engineering & structural dynamics*, 9(3), pp.251-262.
- [9] Tsai, H.C. and Lin, G.C., 1993. Optimum tuned-mass dampers for minimizing steady-state response of support-excited and damped systems. *Earthquake engineering & structural dynamics*, 22(11), pp.957-973.
- [10] Sadek, F., Mohraz, B., Taylor, A.W. and Chung, R.M., 1997. A method of estimating the parameters of tuned mass dampers for seismic applications. *Earthquake Engineering & Structural Dynamics*, 26(6), pp.617-635.
- [11] Miah, M.S., Miah, M. and Hossain, M., 2019. Development and Performance Evaluation of a Novel Translational Tuned Mass Damper. *In International Journal of Engineering Research in Africa* (Vol. 45, pp. 53-73). Trans Tech Publications Ltd.
- [12] Murudi, M.M. and Mane, S.M., 2004, August. Seismic effectiveness of tuned mass damper (TMD) for different ground motion parameters. *In 13th World Conference on Earthquake Engineering*.
- [13] Bekdaş, G. and Nigdeli, S.M., 2013. Mass ratio factor for optimum tuned mass damper strategies. *International Journal of Mechanical Sciences*, 71, pp.68-84.
- [14] Qin, L., Yan, W.M., & Guo, S.B. (2011). Numerical Study of a New Variable Friction TMD. *Advanced Materials Research*, 243-249, 5450-5457.
- [15] Farghaly, A.A. and Salem Ahmed, M., 2012. Optimum design of TMD system for tall buildings. *ISRN Civil Engineering*, 2012.
- [16] Kang, Y.J. and Peng, L.Y., 2019. Optimisation Design and Damping Effect Analysis of Large Mass Ratio Tuned Mass Dampers. *Shock and Vibration*, 2019.
- [17] Etedali, S. and Rakhshani, H., 2018. Optimum design of tuned mass dampers using multi-objective cuckoo search for buildings under seismic excitations. *Alexandria engineering journal*, 57(4), pp.3205-3218.
- [18] Mohebbi, M. and Joghataie, A., 2012. Designing optimal tuned mass dampers for nonlinear frames by distributed genetic algorithms. *The Structural Design of Tall and Special Buildings*, 21(1), pp.57-76.
- [19] Hervé Poh'sié, G., Chisari, C., Rinaldin, G., Fragiaco, M., Amadio, C. and Ceccotti, A., 2016. Application of a translational tuned mass damper designed by means of genetic algorithms on a multistory cross-laminated timber building. *Journal of Structural Engineering*, 142(4), p.E4015008.
- [20] Connor, J.J., 2003. Structural Motion Control (p. 220). Pearson Education, Inc., New Jersey, USA.
- [21] Banerjee, S. and Ghosh, A.D., 2020, September. Optimal Design of Tuned Mass Damper for Base-Excited Structures. *In IOP Conference Series: Materials Science and Engineering* (Vol. 936, No. 1, p. 012016). IOP Publishing.
- [22] Lagarias, J.C., Reeds, J.A., Wright, M.H. and Wright, P.E., 1998. Convergence properties of the Nelder-Mead simplex method in low dimensions. *SIAM Journal on optimization*, 9(1), pp.112-147.